JCTC Journal of Chemical Theory and Computation

Ab Initio Study of Spin-Vibronic Dynamics in the Ground $\tilde{X}^2E$ and Excited $\tilde{A}^2A_1$ Electronic States of $CH_3S^\bullet$

Aleksandr V. Marenich and James E. Boggs*

Institute for Theoretical Chemistry, Department of Chemistry and Biochemistry, The University of Texas at Austin, 1 University Station A5300, Austin, Texas 78712

Received June 6, 2005

Abstract: A spin-vibronic Hamiltonian including the linear, quadratic, cubic, and quartic Jahn−Teller terms with account for all important anharmonic effects was applied to study electronic and nuclear dynamics in the ground $\tilde{X}^2E$ and first excited $\tilde{A}^2A_1$ electronic states of the CH_3S methylthio radical (C_{3v}). The $E\otimes(3a_1+3e)$ problem of spin-vibronic eigenvalues and eigenfunctions was solved in a basis set of products of electronic, electron spin, and vibrational functions. The Jahn−Teller distortions in $\tilde{X}^2E$ CH_3S are totally quenched by the strong spin−orbit coupling. However, Jahn−Teller interaction terms in the spin-vibronic Hamiltonian cannot be neglected for the high precision evaluation of energy levels of CH_3S. The results of calculations show the importance of inclusion of at least quadratic vibronic terms into variational treatment. The nonadiabatic (pseudo-Jahn−Teller) coupling of the $\tilde{X}^2E$ and $\tilde{A}^2A_1$ electronic states was found small and safely removable from the spin-vibronic Hamiltonian of CH_3S.

Introduction

This paper is intended to extend our previous study[1] of the Jahn−Teller (JT) effect and spin−orbit coupling (SOC) in the ground electronic state $\tilde{X}^2E$ of the methylthio (CH_3S) radical by means of a variational solution of the E⊗e problem using ab initio methods to parametrize the Hamiltonian. The formalism of our calculations is described in detail in refs 2 and 3. The ground $\tilde{X}^2E$ electronic state of CH_3S was studied here with the simultaneous treatment of spin−orbit coupling, all linear and quadratic JT interactions including multimode couplings, the cubic and most important quartic vibronic terms, and all significant anharmonic effects. Eigenenergies and eigenfunctions of a model spin-vibronic Hamiltonian were calculated in a basis set of products of electronic, electron spin, and vibrational functions transformed according to irreducible representations ($E_{3/2}$ and $E_{1/2}$) of the double C_{3v} symmetry group.[4,5]

A study of the nuclear dynamics in the first excited $\tilde{A}^2A_1$ state of CH_3S within the adiabatic approximation[4] was also performed. The smallness of nonadiabatic coupling between the ground $\tilde{X}^2E$ and excited $\tilde{A}^2A_1$ electronic states was proven with calculation of linear vibronic constants responsible for the pseudo-Jahn−Teller (PJT) effect[6] in CH_3S. The equilibrium geometry and force constants, vibrational energy levels in $\tilde{A}^2A_1$ CH_3S, and energies (T_e and T_o) of the $\tilde{A}^2A_1 \leftrightarrow \tilde{X}^2E$ electronic transition were found.

Details of Computations

Calculations of the Spin-Vibronic Dynamics in $\tilde{X}^2E$ CH_3S. The model Hamiltonian describing the dynamics of electrons and nuclei in $\tilde{X}^2E$ CH_3S (refs 2 and 3) is obtained with use of refs 7 and 8 in terms of the spin-vibronic matrix that is formed in the basis set of four spin-electronic functions $X = |\Lambda\rangle\ |\Sigma\rangle$: $|-1\rangle|-^1/_2\rangle$, $|+1\rangle|-^1/_2\rangle$, $|-1\rangle|+^1/_2\rangle$, and $|+1\rangle|+^1/_2\rangle$, where the label $\Lambda = \pm 1$ is intended to distinguish the two components of the E-term, lowest (−1) and upper (+1), and the value of $\Sigma = \pm^1/_2$ is a projection of the electron spin ($S = {}^1/_2$) on the symmetry axis of the molecule

$$\begin{pmatrix} (\hat{T} + V_E^{\circ} \mp \Delta_{SO}) - E & V_{-+} \\ V_{+-} & (\hat{T} + V_E^{\circ} \pm \Delta_{SO}) - E \end{pmatrix} \begin{pmatrix} X_{\Lambda=-1\Sigma=\mp(1/2)} \\ X_{\Lambda=+1\Sigma=\mp(1/2)} \end{pmatrix} = 0 \quad (1)$$

where $V_E^{\circ} = \langle \pm 1|\hat{V}(r,Q)|\pm 1\rangle$ and $2\Delta_{SO}$ is the value of spin−orbit splitting ($-A_{SO}\zeta_e$) at the electronic degeneracy point

* Corresponding author e-mail: james.boggs@mail.utexas.edu.

10.1021/ct0501452 CCC: $30.25
Published on Web 09/28/2005

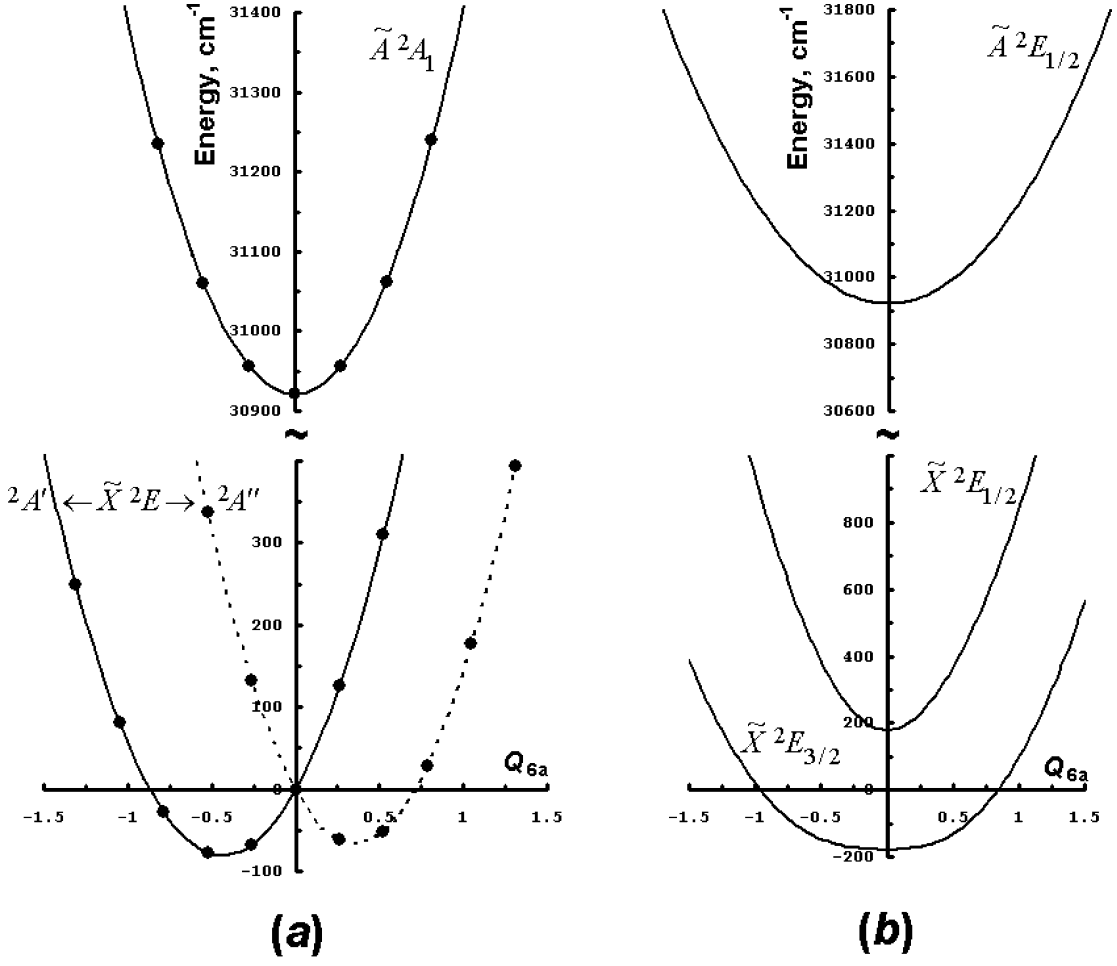

Figure 1. Vertical energies for $\tilde{X}^2E$ and $\tilde{A}^2A_1$ CH_3S without spin−orbit coupling (a) and with SOC (b) projected on the normal mode Q_6(E). Ab initio single point energies calculated by EOMIP/aug-cc-pCVTZ are depicted with solid circles. The a component of Q_6 is dimensionless. Other normal coordinates **Q** (**S** = **LQ**) were equal to zero. The **L**-matrix was calculated at the C_{3v} symmetry nuclear configuration optimized for the $\tilde{X}^2E$ state.

(Q_0), r and Q are electronic and nuclear coordinates, respectively, $\hat{V}(r,Q)$ is the electrostatic potential involving electrons and nuclei, $\hat{T}(Q)$ is the nuclear kinetic energy operator. In case of $\Delta_{SO} = 0$, diagonalization of eq 1 at different nuclear configurations gives two adiabatic potential surfaces (A′ and A″) crossing at Q_0 (Figure 1, part a). With inclusion of the spin−orbit coupling ($\Delta_{SO} \neq 0$), the two surfaces corresponding to the two spin−orbit states of $E_{3/2}$ (lower) and $E_{1/2}$ (upper) symmetry avoid crossing (Figure 1, part b).

There are six normal coordinates (Q) determined for the C_{3v} symmetry nuclear configuration of CH_3S: symmetric CH_3-stretching $Q_1(A_1)$, symmetric CH_3-deformation $Q_2(A_1)$ ("umbrella"), CS-stretching $Q_3(A_1)$, asymmetric CH_3-stretching Q_4(E), and asymmetric HCH− ("scissors") and HCS-deformations, Q_5(E) and Q_6(E), respectively. The electronic matrix (V) elements in eq 1 are expressed via the complex $Q_\pm = Q_a \pm (-1)^{1/2}Q_b$ components of doubly degenerate normal modes Q(E) as

$$V_E^{\,o} = \sum_{i=1}^{3}\frac{1}{2}\omega_i Q_i^{\,2} + \sum_{i=4}^{6}\frac{1}{2}\omega_i Q_{i+}Q_{i-} + \Delta V_{anh} \qquad (2)$$

and

$$V_{\pm\mp} = \sum_{i=4}^{6} k_i Q_{i\mp} + \sum_{i=4}^{6}\frac{1}{2} g_{ii} Q_{i\pm}^{\,2} + \sum_{i=4}^{6}\sum_{j=i+1}^{6} g_{ij} Q_{i\pm} Q_{j\pm} + \sum_{i=1}^{3}\sum_{j=4}^{6} b_{ij} Q_i Q_{j\mp} + V_{\pm\mp}(\mathrm{III}) + V_{\pm\mp}(\mathrm{IV}) \quad (3)$$

The quantities ω_i in eq 2 refer to harmonic frequencies calculated for the three nondegenerate and three 2-fold degenerate vibrational modes. The potential term ΔV_{anh} is responsible for anharmonic effects.

The vibronic term $V_{\pm\mp}$ in eq 3 includes Jahn−Teller parameters of up to the fourth order. The functions $V_{\pm\mp}$(III) and $V_{\pm\mp}$(IV) worked out in detail[3] refer to cubic and quartic vibronic couplings, respectively. The linear (k_i), quadratic (g_{ij}), cubic (g_{ijk}), and quartic (g_{ijkl}) vibronic constants (see also eqs 6−8 in ref 3) mix electronic states $\Lambda = \pm 1$ via single JT active vibrations or via their combinations. Other quadratic, cubic, and quartic constants of type "b" are responsible for the vibronic coupling between nondegenerate ($i = 1-3$) and JT active ($j = 4-6$) vibrational modes in

CH_3S. All the constants of *i*, *ij*, *ijk*, and *iijj* type were considered here.

The term ΔV_{anh} in eq 2 was expressed via the symmetrized Taylor series:

$$\Delta V_{anh} = \sum_{i=1}^{3}\frac{1}{3!}f_{iii}Q_i^3 + \sum_{i=1}^{3}\sum_{j=i+1}^{3}\frac{1}{2!}f_{iij}Q_i^2Q_j + \sum_{i=1}^{3}\sum_{j=i+1}^{3}\frac{1}{2!}f_{ijj}Q_iQ_j^2 + \sum_{i=1}^{3}\sum_{j=i+1}^{3}\sum_{k=j+1}^{3}f_{ijk}Q_iQ_jQ_k + \sum_{i=4}^{6}\frac{1}{3!2}f_{iii}(Q_{i+}^3 + Q_{i-}^3) + \sum_{i=4}^{6}\sum_{j=i+1}^{6}\frac{1}{2!2}f_{iij}(Q_{i+}^2Q_{j+} + Q_{i-}^2Q_{j-}) + \sum_{i=4}^{6}\sum_{j=i+1}^{6}\frac{1}{2!2}f_{ijj}(Q_{i+}Q_{j+}^2 + Q_{i-}Q_{j-}^2) + \sum_{i=4}^{6}\sum_{j=i+1}^{6}\sum_{k=j+1}^{6}\frac{1}{2}f_{ijk}(Q_{i+}Q_{j+}Q_{k+} + Q_{i-}Q_{j-}Q_{k-}) + \sum_{i=1}^{3}\sum_{j=4}^{6}\frac{1}{2!}f_{ijj}Q_iQ_{j+}Q_{j-} + \sum_{i=1}^{3}\sum_{j=4}^{6}\sum_{k=j+1}^{6}\frac{1}{2}f_{ijk}Q_i(Q_{j+}Q_{k-} + Q_{j-}Q_{k+}) + \sum_{i=1}^{3}\frac{1}{4!}f_{iiii}Q_i^4 + \sum_{i=1}^{3}\sum_{j=i+1}^{3}\frac{1}{2!2!}f_{iijj}Q_i^2Q_j^2 + \sum_{i=4}^{6}\frac{1}{4!}f_{iiii}Q_{i+}^2Q_{i-}^2 + \sum_{i=4}^{6}\sum_{j=i+1}^{6}\frac{1}{2!2!}f_{iijj}Q_{i+}Q_{j+}Q_{i-}Q_{j-} + \sum_{i=1}^{3}\sum_{j=4}^{6}\frac{1}{2!2!}f_{iijj}Q_i^2Q_{j+}Q_{j-} \quad (4)$$

where the quantities f_{iii}, f_{ijj}, and f_{ijk} are cubic force constants (the integers *i* and *j* run over all vibrations). The coefficients f_{iiii} and f_{iijj} refer to quartic constants. The force constants of higher order are found to be small and can be omitted.

The general variational solution of eq 1 was obtained in a basis set of products of electronic, electron spin, and vibrational functions transformed according to irreducible representations ($E_{3/2}$ and $E_{1/2}$) of the double C_{3v} symmetry group[4,5] (relativistic symmetry). In the absence of SOC, the vibronic eigenfunctions obviously comply to irreducible representations (A_1, A_2, and E) of the C_{3v} group (nonrelativistic symmetry). The vibrational portion of the basis set consists of the orthonormalized harmonic oscillator eigenfunctions expressed via Hermite polynomials.[4]

Calculations of the Nuclear Dynamics in $\tilde{A}^2A_1$ CH_3S with Use of the Adiabatic Approximation. The nuclear dynamics in the first excited electronic state $\tilde{A}^2A_1$ was studied with the model vibrational Hamiltonian written in terms of the one-dimensional harmonic oscillator for symmetric normal modes $Q_1(A_1)$, $Q_2(A_1)$, and $Q_3(A_1)$ and the two-dimensional (isotropic) harmonic oscillator for asymmetric modes $Q_4(E)$, $Q_5(E)$, and $Q_6(E)$[4]

$$\hat{H} = \sum_{i=1}^{3}\frac{1}{2}\omega_i\left(-\frac{\partial^2}{\partial Q_i^2} + Q_i^2\right) + \sum_{i=4}^{6}\frac{1}{2}\omega_i\left(-\frac{\partial^2}{\partial Q_{i+}\partial Q_{i-}} + Q_{i+}Q_{i-}\right) + \Delta V_{anh} \quad (5)$$

where the potential term ΔV_{anh} expressed in eq 4 accounts for anharmonic effects in $\tilde{A}^2A_1$ CH_3S. The dimensionless normal coordinates were used in eqs 1−5.

Eigenenergies and eigenfunctions of eq 5 are calculated in a basis set of products of the one- or two-dimensional harmonic oscillator eigenfunctions[4] transformed according to irreducible representations (A_1, A_2, and E) of the C_{3v} point symmetry group.[4,5]

Miscellaneous Details on Calculation of Model Parameters. Optimizations of geometry parameters and harmonic analyses of the C_{3v} symmetry nuclear configurations in the $\tilde{X}^2E$ and $\tilde{A}^2A_1$ electronic states of CH_3S were performed numerically using the symmetry-adapted internal coordinates **S** related to the normal coordinates as $\mathbf{S} = \mathbf{L}\,\mathbf{Q}$ (see ref 1) and the program ANOCOR[9] for generation of distorted geometries and harmonic analysis. The unperturbed (diabatic) harmonic frequencies $\omega_4(E)$, $\omega_5(E)$, and $\omega_6(E)$ in $\tilde{X}^2E$ CH_3S were calculated by differentiation of the function $V_E^\circ(Q) = {}^1/_2(U_+ + U_-)$ averaged over total energies of the upper (U_+) and lower (U_-) adiabatic electronic states arising from the degenerate $\tilde{X}^2E$ term.

The vibrational and vibronic parameters from eqs 3 and 4 were found through the least-squares fit of model potential energy values to "exact" ab initio energies for the two components of $\tilde{X}^2E$ and for the $\tilde{A}^2A_1$ state over 1153 nuclear configurations distorted on the normal coordinates Q_i and Q_{ja} ($i = 1-3$, $j = 4-6$) (see details in refs 2 and 3). For the ab initio calculations of single point energies, we used the equation-of-motion coupled cluster method[10] with the coupled cluster singles and doubles (CCSD) reference wave function for the CH_3O^- -anion ground state (further abbreviated to EOMIP) and with the augmented correlation consistent polarized valence basis sets of Dunning et al.[11] of triple-ζ quality including extra functions[12] for C and S to account for core−core and core-valence correlation (further abbreviated to aug-cc-pCVTZ). The EOMIP calculations were performed with a local version of the ACES II program package.[13]

The value of spin−orbit splitting ($-A_{SO}\xi_e = 358\ cm^{-1}$) at the electronic degeneracy point (C_{3v}) in $\tilde{X}^2E$ CH_3S has been found in our previous study[1] with the use of multiconfiguration quasi-degenerate second-order perturbation theory[14] followed by an SOC perturbative calculation within the full Breit-Pauli spin−orbit operator.[15] This spin−orbit calculation was performed with the GAMESS (US) package.[16]

Evaluation of the Nonadiabatic Coupling of the Ground $\tilde{X}^2E$ and First Excited $\tilde{A}^2A_1$ Electronic States. To study the role of the pseudo-Jahn−Teller interaction between the electronic states of interest, we constructed a diabatic electronic matrix relevant to the $(E+A_1)\otimes e$ problem to introduce the nonadiabatic coupling of three states by means of generalization of findings in refs 17−19

$$V = \begin{pmatrix} V_E^{\,o} \mp \Delta_{SO} & V_{-+}^{\,JT} & \frac{1}{\sqrt{2}}V_{+-}^{\,PJT} \\ V_{+-}^{\,JT} & V_E^{\,o} \pm \Delta_{SO} & -\frac{1}{\sqrt{2}}V_{-+}^{\,PJT} \\ \frac{1}{\sqrt{2}}V_{-+}^{\,PJT} & -\frac{1}{\sqrt{2}}V_{+-}^{\,PJT} & V_{A_1}^{\,o} \end{pmatrix} \quad (6)$$

where the diabatic potentials $V_E^\circ(Q)$ and $V_{A_1}^\circ(Q)$ are

expressed with use of eqs 2 and 4 in terms of normal coordinates Q_i ($i = 1-3$) and $Q_{i\pm} = Q_{ia} \pm (-1)^{1/2}Q_{ib}$ ($i = 4-6$) corresponding to the ground $\tilde{X}^2E$ state of CH_3S. The value of $T_v = V_{A_1}^{\circ}(0) - V_E^{\circ}(0)$ is the vertical energy of the $\tilde{A}^2A_1 \leftrightarrow \tilde{X}^2E$ transition. The Jahn−Teller and pseudo-Jahn−Teller coupling constants $V_{\pm\mp}(Q)$ are expressed with use of eq 3. As in eq 1, the electronic term V_E° in eq 6 may undergo spin−orbit splitting of $2\Delta_{SO}$. Diagonalization of eq 6 at $\Delta_{SO} = 0$ and $Q_b = 0$ leads to the three adiabatic potentials $U_{E(A')}$, $U_{E(A)}$, and U_{A_1} representing ab initio total energies (Figure 1, part a):

$$U_{E(A'')} = V_E^{\circ} + A_{JT} \tag{7}$$

$$U_{E(A')} = \frac{1}{2}(V_{A_1}^{\circ} + V_E^{\circ} - A_{JT} - \sqrt{4A_{PJT}^2 + (V_{A_1}^{\circ} - V_E^{\circ} + A_{JT})^2}) \tag{8}$$

$$U_{A_1} = \frac{1}{2}(V_{A_1}^{\circ} + V_E^{\circ} - A_{JT} + \sqrt{4A_{PJT}^2 + (V_{A_1}^{\circ} - V_E^{\circ} + A_{JT})^2}) \tag{9}$$

The functions of A_{JT} and A_{PJT} are defined as $V_{+-}^{(P)JT}(Q_a) = V_{-+}^{(P)JT}(Q_a)$. Taking into account only linear vibronic (JT and PJT) coupling, one can readily represent the expressions for these potentials given by Woywod et al.[17] in the study of the Jahn−Teller and pseudo-Jahn−Teller interactions in the ammonia cation (cf. eqs 2.17 in ref 17 following the phase convention for the choice of a sign on λ).

In the case of well-separated adiabatic states with $4A_{PJT}^2 \ll (V_{A_1}^{\circ} - V_E^{\circ} + A_{JT})^2$, eqs 8 and 9 can be reduced to

$$U_{E(A')} = V_E^{\circ} - A_{JT} - \frac{A_{PJT}^2}{T_v} \tag{10}$$

$$U_{A_1} = V_{A_1}^{\circ} + \frac{A_{PJT}^2}{T_v} \tag{11}$$

with the further simplification $V_{A_1}^{\circ} - V_E^{\circ} + A_{JT} \approx T_v = V_{A_1}^{\circ}(0) - V_E^{\circ}(0)$. Thus, even linear pseudo-Jahn−Teller effect ($A_{PJT} \sim \lambda Q_a$) giving a quadratic contribution to the adiabatic potentials $U_{E(A')}$ and U_{A_1} may cause an additional instability of the high-symmetry nuclear configuration with reduction of the curvature of the low sheet.[20] According to eqs 10 and 11, a pseudo-Jahn−Teller coupling may be heavily quenched with a large value of the vertical energy T_v (a case of well-separated states). If $(A_{PJT}^2/T_v) \approx 0$, the expressions for the adiabatic potentials (eqs 10 and 11) are reduced to the formulas for uncoupled electronic states ($E = A' + A''$ and A_1) which can be treated individually by use of eqs 1 and 5.

The linear pseudo-Jahn−Teller constants λ_4, λ_5, and λ_6 which couple these electronic states via the terms $V_{\pm\mp}^{PJT} = \sum_{i=4}^{6}\lambda_i Q_{i\mp}$ in eq 6 were evaluated numerically by means of EOMIP/aug-cc-pCVTZ single point calculations with use of eqs 7−9 and $A_{PJT} = \sum_{i=4}^{6}\lambda_i Q_{ia}$. A variational solution of the spin-vibronic Hamiltonian with inclusion of the PJT coupling of the $\tilde{X}^2E$ and $\tilde{A}^2A_1$ states was beyond the scope of the present study.

Results of Calculations and Discussion

The Ground $\tilde{X}^2E$ Electronic State of CH_3S. As predicted by the Jahn−Teller theorem,[6] the C_{3v} symmetry nuclear configuration in the $\tilde{X}^2E$ ground electronic state of CH_3S is unstable as shown in Figure 1(a) (no spin−orbit coupling included). There are two specific points on the adiabatic potential energy surface (PES) of $\tilde{X}^2E$ CH_3S corresponding to distorted (C_s symmetry) nuclear configurations (a minimum and a saddle point) with electron wave functions of A′ or A″ symmetries. The Jahn−Teller stabilization energy $E_{JT} = 92$ cm^{-1} is determined as $E_{JT} = U(C_{3v}, E) - U(C_s, A')$ where $U(C_{3v}, E)$ and $U(C_s, A')$ are total energies corresponding to the $C_{3v}(E)$ and $C_s(A')$ equilibrium geometries, respectively. The barrier to pseudorotation or the quadratic Jahn−Teller stabilization energy is $\Delta_{JT} = U(C_s, A'') - U(C_s, A')$, $\Delta_{JT} = 15$ cm^{-1}.

After account for the spin−orbit coupling, the shape of adiabatic potential surfaces of $\tilde{X}^2E$ CH_3S is changed dramatically as shown in Figure 1(b). The value of spin−orbit splitting in $\tilde{X}^2E$ CH_3S ($-A_{SO}\zeta_e = 358$ cm^{-1}) is significantly larger than the Jahn−Teller stabilization energy $E_{JT} = 92$ cm^{-1}. As shown by our previous calculations,[1] the strong spin−orbit coupling totally quenches the Jahn−Teller distortions in the ground electronic state of CH_3S (Figure 1, part b). Instead of the three equivalent minima corresponding to the Jahn−Teller distorted geometries on the lower potential energy surface of $\tilde{X}^2E$ CH_3S (the Mexican hat[6]) as depicted in Figure 2(a), there is a minimum at the C_{3v} symmetry nuclear configuration (Figure 2, part b). The reduction of the Jahn−Teller effect by spin−orbit coupling does *not* mean though that the vibronic effects may be completely neglected.[7] The shape of potential surfaces for the two final spin−orbit states is determined by the relation between the $A_{SO}\zeta_e$ quantity and the values of E_{JT} and Δ_{JT}. Hence, the thorough evaluation of vibronic parameters and force constants is still important for the most accurate theoretical predictions of spin-vibronic levels of the CH_3S radical.

The EOMIP/aug-cc-pCVTZ values of molecular parameters with inclusion of all significant force constants of higher order and linear, quadratic, cubic, and quartic vibronic constants of $\tilde{X}^2E$ CH_3S are presented in Table 1. The optimal geometry parameters (R_e, α_e), unperturbed harmonic frequencies (ω), and Jahn−Teller stabilization energies (E_{JT}, Δ_{JT}) of $\tilde{X}^2E$ CH_3S (Table 1) are close to results of our previous EOMIP calculations[1] with electronic basis sets of quadruple-ζ quality: $R_e(C-S) = 1.7940$ Å, $R_e(C-H) = 1.0872$ Å, $\alpha_e(HCS) = 109.80°$; $\omega_i = 3066(A_1)$, $1367(A_1)$, $758(A_1)$, $3164(E)$, $1483(E)$, and $938(E)$ cm^{-1} ($i = 1-6$); $E_{JT} = 93.2$ and $\Delta_{JT} = 14.9$ cm^{-1}.[1] Values of linear and quadratic Jahn−Teller constants calculated in ref 1 ($k_4 = -90$, $k_5 = -166$, $k_6 = -372$, $g_{44} = 0.25$, $g_{55} = -24$, and $g_{66} = 93$ cm^{-1}) are also similar to relevant numbers presented in Table 1. Hence, further extension of the basis set would be expected to improve our results only a little. The large magnitudes of force constants corresponding to the CH_3-stretchings $Q_1(A_1)$ and $Q_4(E)$ indicate that these vibrations exhibit the most pronounced anharmonicity. Calculations of diagonal vibronic constants with the use of multiconfiguration quasi-degenerate second-order perturbation theory result in the values ($k_4 =$

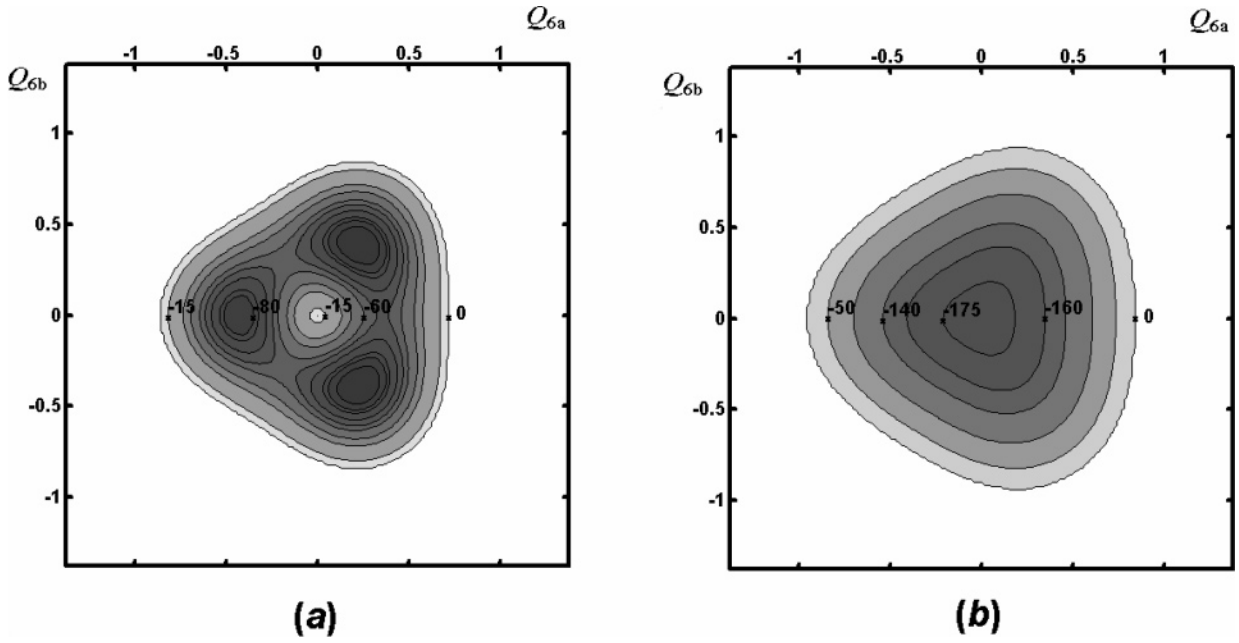

Figure 2. The map of the potential energy surface of $\tilde{X}^2E$ CH_3S (the low sheet) without spin−orbit coupling (a) and with SOC (b) for the normal mode Q_6(E). Energies are given in cm^{-1}. The a and b components of Q_6 are dimensionless.

Table 1. Structure and Spin-Vibronic Parameters of CH_3S in the Ground $\tilde{X}^2E$ and First Excited $\tilde{A}^2A_1$ Electronic States[a]

			$\tilde{X}^2E$ CH_3S		
$E_{JT} = 92$	$\Delta_{JT} = 15$	$-A_{SO}\zeta_e = 358$	R_e(C−S) = 1.7944	R_e(C−H) = 1.0880	α_e(HCS) = 109.79
$\omega_1(A_1) = 3062$	$\omega_2(A_1) = 1373$	$\omega_3(A_1) = 752$	$\omega_4(E) = 3157$	$\omega_5(E) = 1490$	$\omega_6(E) = 943$
$f_{111} = -1067$	$f_{222} = 136$	$f_{333} = -251$	$f_{444} = 823$	$f_{555} = 77$	$f_{666} = -32$
$f_{1111} = 330$	$f_{2222} = -20$	$f_{3333} = 73$	$f_{4444} = 578$	$f_{5555} = -25$	$f_{6666} = 35$
$k_4 = -90$	$k_5 = -168$	$k_6 = -369$	$g_{44} = -7$	$g_{55} = -28$	$g_{66} = 98$
$g_{444} = -1$	$g_{555} = -25$	$g_{666} = -25$	$g_{4444} = 2$	$g_{5555} = -6$	$g_{6666} = -0.02$
$g_{45} = -5$	$g_{46} = 34$	$g_{56} = -43$	$b_{14} = 3$	$b_{15} = 11$	$b_{16} = -25$
$b_{24} = 24$	$b_{25} = -38$	$b_{26} = 52$	$b_{34} = 8$	$b_{35} = 25$	$b_{36} = 64$
			$\tilde{A}^2A_1$ CH_3S		
$T_e = 27308$			R_e(C−S) = 2.0643	R_e(C−H) = 1.0794	α_e(HCS) = 99.75
$\omega_1(A_1) = 3124$	$\omega_2(A_1) = 1203$	$\omega_3(A_1) = 465$	$\omega_4(E) = 3299$	$\omega_5(E) = 1454$	$\omega_6(E) = 718$
$f_{111} = -1070$	$f_{222} = 217$	$f_{333} = -161$	$f_{444} = 833$	$f_{555} = 170$	$f_{666} = -23$
$f_{1111} = 312$	$f_{2222} = -18$	$f_{3333} = 66$	$f_{4444} = 545$	$f_{5555} = -14$	$f_{6666} = 33$

[a] Values and dimensions: distances R (Å), valence angles α (deg), all remaining quantities are in cm^{-1}. The values of geometric parameters (R and α), unperturbed harmonic frequencies (ω), force (f) and vibronic (k, g, b) constants were found numerically by means of EOMIP/aug-cc-pCVTZ total energy calculations over 1153 single points. The off-diagonal force (f) and vibronic (g and b) constants of *ijj*, *ijk*, and *iijj* type were small (with the exception of $f_{144} = -1131$, $f_{1144} = 358$ cm^{-1} for $\tilde{X}^2E$ and $f_{144} = -1137$, $f_{1144} = 335$ cm^{-1} for $\tilde{A}^2A_1$) and were omitted here (but still included in our dynamical calculations). The magnitude of $-A_{SO}\zeta_e$ shows the spin−orbit splitting of the $\tilde{X}^2E$ state.[1] The Jahn−Teller stabilization energy and barrier to pseudorotation are $E_{JT} = U(C_{3v}, E) - U(C_s, A')$ and $\Delta_{JT} = U(C_s, A'') - U(C_s, A')$, respectively. The value of T_e is an adiabatic energy of the $\tilde{A}^2A_1 \leftrightarrow \tilde{X}^2E_{3/2}$ transition.

-91, $k_5 = -154$, $k_6 = -385$, $g_{44} = -10$, $g_{55} = -29$, and $g_{66} = 102$ cm^{-1}) that are close to the ones obtained by EOMIP (Table 1). The values of Jahn−Teller stabilization energies E_{JT} and Δ_{JT} were calculated considering Jahn−Teller coupling of different orders. The inclusion of only linear constants reproduces the ab initio value of E_{JT} relatively poorly (82 cm^{-1}), whereas the addition of quadratic constants improves the quality of the model ($E_{JT} = 91$ and $\Delta_{JT} = 14$ cm^{-1}). Accounting for the cubic terms reproduces the ab initio values of $E_{JT} = 92$ and $\Delta_{JT} = 15$ cm^{-1} exactly, as shown in Table 1, and further addition of the quartic JT constants produces no further change.

To study the role of Jahn−Teller coupling of different orders, we performed a solution of the E⊗2e eigenvalue problem for $\tilde{X}^2E$ CH_3S (Table 2) with inclusion of two vibrational coordinates only: asymmetric HCH- and HCS-deformation normal modes, Q_5(E) and Q_6(E), respectively. The Q_5(E) and Q_6(E) modes, strongly coupled together, are almost solely responsible for the Jahn−Teller effect in $\tilde{X}^2E$ CH_3S, whereas the linear and quadratic vibronic couplings predicted for the asymmetric CH_3-stretching Q_4(E) are smaller than for Q_5(E) and Q_6(E) (compare k_4 and g_{44} with k_5 and g_{55} or with k_6 and g_{66} in Table 1). The spin-vibronic eigenstates were approximately assigned in terms of single normal oscillators. The eigenvalues of the model spin-vibronic Hamiltonian for $\tilde{X}^2E$ CH_3S calculated within the fourth-order vibronic coupling (eq 3, Table 2) are expected to be the most accurate energies in Table 2. The exclusion of all the quartic Jahn−Teller constants (the third-order vibronic coupling) does not lead to a noticeable loss of the

Table 2. Low Spin-Vibronic Energy (in cm^{-1}) Levels in $\tilde{X}^2E$ CH_3S Assigned to the Normal Modes Q_5 and Q_6 (E⊗2e Problem)[a]

assignment		first order	second order	third order	fourth order
0_0(e)	$e_{3/2}^-$	0	0	0	0
0_0(e*)	$e_{1/2}^+$	262	261	255	255
6_1(a_1)	$e_{1/2}^-$	848	818	804	804
6_1(a_2)	$e_{1/2}^+$	1066	1107	1088	1088
6_1(e)	$e_{1/2}^-$	1109	1102	1103	1104
6_1(e*)	$e_{3/2}^+$	1266	1257	1240	1241
5_1(a_1)	$e_{1/2}^-$	1466	1457	1451	1452
5_1(e)	$e_{1/2}^-$	1479	1487	1483	1484
6_2(e)	$e_{1/2}^-$	1730	1692	1670	1671
5_1(e*)	$e_{3/2}^+$	1704	1710	1688	1691
5_1(a_2)	$e_{1/2}^+$	1724	1713	1698	1699
6_2(e*)	$e_{3/2}^+$	1938	1861	1846	1846
6_2(e)	$e_{3/2}^-$	1986	2060	2045	2045
6_2(e*)	$e_{1/2}^+$	2071	2111	2082	2083
6_2(a_1)	$e_{1/2}^-$	2169	2146	2133	2136
6_2(a_2)	$e_{1/2}^+$	2250	2246	2226	2227

[a] Calculations were performed with inclusion of all linear (vibronic coupling of first order), all quadratic (second order), all cubic (third order), and quartic vibronic (fourth order) constants with the use of $-A_{SO}\zeta_e = 2\Delta_{SO} = 358$ cm^{-1} for eq 1. Occupation quantum numbers for the rest of the vibrational modes were equal to zero. The eigenstates were approximately correlated to vibronic states. The symmetry of spin-vibronic levels ($e_{3/2}$ or $e_{1/2}$) complies to the following rules: $E_{1/2}⊗e = e_{3/2} + e_{1/2}$ and $E_{1/2}⊗a_1 = E_{1/2}⊗a_2 = e_{1/2}$, where the symmetry of an electronic spin function ($S = 1/2$) is $E_{1/2}$ and the symmetries of vibronic levels are a_1, a_2, e (e* denotes another component of a doubly degenerate level). The sign −(+) indicates an assignment of a spin-vibronic level to the lower $\tilde{X}^2E_{3/2}$ (upper $\tilde{X}^2E_{1/2}$) spin−orbit state.

accuracy of eigenvalues at least for the lowest ones. The inaccuracy of eigenenergies calculated after exclusion of all the cubic and quartic vibronic terms from eq 3 varies in the range of 2−28 cm^{-1} for values of Table 2 (the second-order vibronic coupling). The error caused by omission of all the vibronic parameters except linear (the first-order coupling) is 5−92 cm^{-1}. Therefore, the quartic vibronic terms in the spin−orbit Hamiltonian for $\tilde{X}^2E$ CH_3S are quite small (Table 1) and can be neglected even for calculations of higher energy levels without a significant loss of accuracy. The inclusion of cubic vibronic constants is still desirable for a benchmark calculation of the spin-vibronic spectrum of CH_3S. On the other hand, the evaluation of thermochemical properties of CH_3S can be performed with eigenvalues of lower accuracy (the second-order or even first-order vibronic coupling, Table 2). This conclusion is in agreement with our previous result obtained for $\tilde{X}^2E$ CH_3O.[3] The spin−orbit splitting in $\tilde{X}^2E$ CH_3S ($-A_{SO}\zeta_e = 358$ cm^{-1}) is much larger than in $\tilde{X}^2E$ CH_3O (134 cm^{-1}).[2,3] The Jahn−Teller effect in $\tilde{X}^2E$ CH_3S ($E_{JT} = 92$ cm^{-1}) is rather weaker than in $\tilde{X}^2E$ CH_3O ($E_{JT} = 270$ cm^{-1}), and the Jahn−Teller distortions in $\tilde{X}^2E$ CH_3S are totally quenched by a strong spin−orbit coupling (unlike the case[2,3] of $\tilde{X}^2E$ CH_3O). Hence, the spin-vibronic dynamics in CH_3S can be described by means of the vibronic terms of lower order (linear and quadratic for instance), whereas the inclusion of cubic terms in the case of $\tilde{X}^2E$ CH_3O is more vital to a better accuracy.

The large magnitudes of some vibronic constants in Table 1 show the significant Jahn−Teller coupling between different vibrational modes: the constants of g_{ij} type are responsible for vibronic coupling between asymmetric vibrations Q_4(E), Q_5(E), and Q_6(E), whereas the constants b indicate a coupling between nondegenerate ($i = 1-3$) and JT active ($j = 4-6$) vibrations $Q_i(A_1)$ and Q_j(E).

We performed a variational solution of the full E⊗(3e + $3a_1$) eigenvalue problem for $\tilde{X}^2E$ CH_3S with account for all possible vibrational and vibronic couplings of up to the fourth order. Table 3 shows results of calculations of the low spin-vibronic energy levels assigned in terms of single normal oscillators. The calculated energy levels were correlated to one of the two spin−orbit states $^2E_{3/2}$ and $^2E_{1/2}$ arising from the electronic E-term split by SOC. Due to a strong coupling between different normal modes, all the assignments in Table 3 are approximate. For instance, two lowest spin-vibronic eigenstates at 0 and 252 cm^{-1} are definitely correlated to the two spin−orbit components of the lowest vibronic eigenstate. They are made up of the following combinations of basis functions

$$0.93|-\rangle|0_0\rangle + 0.27|+\rangle|6_1, -1\rangle \text{ at } 0\ (e_{3/2}^-) \text{ and}$$
$$0.84|+\rangle|0_0\rangle + 0.45|-\rangle|6_1, 1\rangle \text{ at } 252\ (e_{1/2}^+)\ cm^{-1}$$

where the notation $|-\rangle$ defines the lower spin−orbit state $^2E_{3/2}$ and $|+\rangle$ corresponds to the upper state $^2E_{1/2}$, a function $|6_v, l\rangle$ defines the two-dimensional (isotropic) harmonic oscillator with the principal vibrational quantum number v and the vibrational angular momentum quantum number l ($l = v, v-2, v-4, \ldots$) for a normal mode Q_6(E),[4] the indexes for other vibrational modes are omitted.

The higher energy spin-vibronic levels are more strongly mixed than the lower ones, and their assignments in terms of harmonic oscillators may be more difficult or meaningless. For instance, the spin-vibronic eigenstate at 1826 cm^{-1} (Table 3) is made up of the following combinations only slightly dominated by the basis function $|+\rangle|6_2, 2\rangle$:

$$0.54|+\rangle|6_2,2\rangle + 0.47|+\rangle|5_1,-1\rangle + 0.34|-\rangle|6_3,3\rangle$$
$$-0.29|-\rangle|6_2,0\rangle + 0.28|+\rangle|6_1,-1\rangle + 0.24|-\rangle|5_1,-1\rangle|6_1,1\rangle$$

Hence, the state at 1826 $(e_{3/2}^+)$ cm^{-1} can be approximately assigned to the upper spin−orbit component of the doubly degenerate vibronic level 6_2(e) arising from a two-quantum vibrational excitation of the normal oscillator corresponding to the asymmetric HCS-deformation Q_6(E).

The role of inclusion of the vibronic coupling between symmetric and Jahn−Teller active normal modes into the spin-vibronic Hamiltonian becomes clear after comparison of results of solutions of the E⊗2e eigenvalue problem (the right column of Table 2) to relevant eigenenergies from Table 3: the difference of these wavenumbers varies from 3 to 24 cm^{-1}. The spin−orbit splitting of the vibronic levels 1_v(e), 2_v(e), and 3_v(e) is a nearly constant value equal to the spin−orbit splitting $-A_{SO}\zeta_e d = 252$ cm^{-1} in the zero vibronic level 0_0(e) because these eigenstates are mostly dominated by a single harmonic oscillator basis function related to a vibrational excitation $1_v(A_1)$, $2_v(A_1)$, or $3_v(A_1)$, respectively, with only a little contribution from 4_v(E), 5_v(E), or 6_v(E). The strong spin−orbit coupling almost totally reduces the vibronic splitting for the eigenstates at 3022($e_{1/2}^-$), 3026($e_{1/2}^-$),

Table 3. Theoretical Spin-Vibronic Energy (in cm^{-1}) Levels in $\tilde{X}^2E$ CH_3S ($E\otimes(3a_1 + 3e)$ Problem) versus Experimental Values[a,b]

assignment	theory	experiment[c]	assignment	theory	experiment[c]
$0_0(e)$	0 ($e_{3/2}^-$)	0	$6_2(e^*)$	1826 ($e_{3/2}^+$)	
$0_0(e^*)$	252 ($e_{1/2}^+$)	256−259,[d] 264 [e]	$3_16_1(e)$	1844 ($e_{1/2}^-$)	
$3_1(e)$	742 ($e_{3/2}^-$)	738−745,[f] 736[e]	$3_16_1(e^*)$	1971 ($e_{3/2}^+$)	
$6_1(a_1)$	793 ($e_{1/2}^-$)	586[d]	$6_2(e)$	2037 ($e_{3/2}^-$)	
$3_1(e^*)$	993 ($e_{1/2}^+$)	980−986,[d] 998[e]	$6_2(e^*)$	2070 ($e_{1/2}^+$)	
$6_1(a_2)$	1078 ($e_{1/2}^+$)		$2_13_1(e)$	2095 ($e_{3/2}^-$)	2045−2057,[f] 2036[e]
$6_1(e)$	1105 ($e_{1/2}^-$)		$6_2(a_1)$	2112 ($e_{1/2}^-$)	
$6_1(e^*)$	1231 ($e_{3/2}^+$)		$2_16_1(a_1)$	2159 ($e_{1/2}^-$)	
$2_1(e)$	1358 ($e_{3/2}^-$)	1325−1332,[f] 1312[e]	$3_15_1(a_1)$	2176 ($e_{1/2}^-$)	
$5_1(a_1)$	1436 ($e_{1/2}^-$)		$3_15_1(e)$	2201 ($e_{1/2}^-$)	2204−2212[d]
$5_1(e)$	1463 ($e_{1/2}^-$)	1489−1501[d]	$6_2(a_2)$	2215 ($e_{1/2}^+$)	
$3_2(e)$	1487 ($e_{3/2}^-$)	1463−1464,[f] 1456[e]	$3_3(e)$	2229 ($e_{3/2}^-$)	2177−2179,[f] 2159[e]
$3_16_1(a_1)$	1540 ($e_{1/2}^-$)		$5_16_1(e)$	2230 ($e_{1/2}^-$)	
$2_1(e^*)$	1613 ($e_{1/2}^+$)	1583−1595,[f] 1559[e]	$5_16_1(e)$	2245 ($e_{3/2}^-$)	
$6_2(e)$	1659 ($e_{1/2}^-$)		$3_26_1(a_1)$	2286 ($e_{1/2}^-$)	
$5_1(e^*)$	1674 ($e_{3/2}^+$)		$2_13_1(e^*)$	2348 ($e_{1/2}^+$)	2310−2319,[f] 2283[e]
$5_1(a_2)$	1680 ($e_{1/2}^+$)		$3_16_2(e)$	2402 ($e_{1/2}^-$)	
$3_2(e^*)$	1734 ($e_{1/2}^+$)	1718−1723,[f] 1713[e]	$3_15_1(e^*)$	2410 ($e_{3/2}^+$)	
$3_16_1(a_2)$	1823 ($e_{1/2}^+$)		$3_15_1(a_2)$	2421 ($e_{1/2}^+$)	

[a] See footnotes to Table 2. [b] All energies are related to the ground level of the lower spin−orbit state $\tilde{X}^2E_{3/2}$. The intervals (in cm^{-1}) calculated for the CH_3-stretchings are 2938 for $1_1(e, e_{3/2}^-)$, 3022 for $4_1(a_1, e_{1/2}^-)$, 3026 for $4_1(e, e_{1/2}^-)$, 3194 for $1_1(e^*, e_{1/2}^+)$, 3275 for $4_1(a_2, e_{1/2}^+)$, and 3282 for $4_1(e^*, e_{3/2}^+)$. See comparison of these wavenumbers to observed intervals in the text. [c] The intervals from the $\tilde{A}^2A_1 \rightarrow \tilde{X}^2E_{3/2}$ and $\tilde{A}^2A_1 \rightarrow \tilde{X}^2E_{1/2}$ laser-induced fluorescence (LIF) spectra of jet-cooled CH_3S observed[21,22] for several pumped bands (0_0^0, 3_0^1, 3_0^2, or 2_0^1) are written here with a hyphen. Tentative assignments are italicized. [d] LIF by Chiang and Lee.[21] [e] LIF by Suzuki, Inoue, and Akimoto.[23] [f] LIF by Misra, Zhu, and Bryant.[22]

$3275(e_{1/2}^+)$, and $3282(e_{3/2}^+)$ cm^{-1} approximately assigned to a single excitation $4_1(e)$ of the asymmetric CH_3-stretching normal mode $Q_4(E)$: a remaining vibronic splitting in the lower spin−orbit component ($E_{3/2}\otimes E = 2e_{1/2}$) and in the upper component ($E_{1/2}\otimes E = e_{3/2} + e_{1/2}$) is 4 and 7 cm^{-1}, respectively, where $E_{3/2}$ ($E_{1/2}$) are relativistic symmetry of a lower (upper) spin−orbit state (see Figure 1, part b).

Theory versus Experiment: the Ground $\tilde{X}^2E$ Electronic State. The CH_3S radical has been studied during the last three decades with use of different spectroscopic techniques (see refs 7 and 21−36 and therein).

In agreement with theory, experiment demonstrates a relatively large spin−orbit splitting of the ground electronic state, in excess of 200 cm^{-1}, and the Jahn−Teller distortions vanish.[7] The theoretical value of spin−orbit splitting in the ground vibronic state of $\tilde{X}^2E$ CH_3S ($-A_{SO}\zeta_e d = 252$ cm^{-1}, Table 3) is close to the observed ones (in cm^{-1}): 220.3[29] (microwave spectroscopy); 259.1,[21] 266,[22] 280 ± 20,[23] and 255.5[30] (laser-induced fluorescence); 280 ± 50[27] and 265 ± 15[34] (photoelectron spectroscopy). The Ham reduction factor d ($d \le 1$) in $-A_{SO}\zeta_e d$ indicates how much the spin−orbit coupling ($-A_{SO}\zeta_e$) is reduced by the Jahn−Teller effect.[7]

Chiang and Lee,[21] Misra et al.,[22] and Suzuki et al.[23] observed the CH_3S $\tilde{X}^2E - \tilde{A}^2A_1$ systems by laser-induced fluorescence (LIF) spectroscopy. The main ($\tilde{X}^2E_{3/2} \rightarrow \tilde{A}^2A_1$) and weak ($\tilde{X}^2E_{1/2} \rightarrow \tilde{A}^2A_1$) progressions detected in the excitation spectrum of CH_3S were assigned to the transitions from the $^2E_{3/2}$ and $^2E_{1/2}$ spin−orbit components of the ground electronic state $\tilde{X}^2E$ CH_3S to different CS-stretching vibrational levels (3^v) of the $^2A_1$ state. Less intense progressions assigned to the $\tilde{X}^2E_{3/2} \rightarrow 2_0^1 3_0^v \tilde{A}^2A_1$ transitions were also identified.[21]

Some intervals for $\tilde{X}^2E_{3/2}$ and $\tilde{X}^2E_{1/2}$ CH_3S observed in the dispersed fluorescence spectra[21−23] are shown in Table 3. The agreement between theory and experiment is good for all the intervals assigned to the symmetric vibrations $Q_2(A_1)$ and $Q_3(A_1)$: deviations vary between 4 and 80 cm^{-1} with the growth for higher energy overtones (Table 3). The interval observed[21] at 1496 ± 6 cm^{-1} (1463 cm^{-1} by theory) in the main progressions $3_0^v\tilde{A}^2A_1 \rightarrow \tilde{X}^2E_{3/2}$, $2_0^1\tilde{A}^2A_1 \rightarrow \tilde{X}^2E_{3/2}$ is assigned to the lower spin−orbit component of the vibronic level $5_1(e)$ (Table 3), but the transition to the upper spin−orbit component (1674 cm^{-1} by theory) was not detected in ref 21 apparently because of the low intensity of relevant lines in the LIF spectrum. Due to a relatively small Jahn−Teller coupling in CH_3S, those lines in the spectrum, which may be assigned to vibrations along the Jahn−Teller active modes, $Q_j(E)$, $j = 4-6$, are likely to be weak,[7] and they may not be detected or identified properly within the experimental accuracy. Some weak lines in the LIF spectrum of CH_3S were *tentatively* assigned by the authors of ref 21 to the symmetric $Q_1(A_1)$ and asymmetric $Q_4(E)$ CH_3-stretchings and the asymmetric HCS-deformation $Q_6(E)$, with $\nu_1(A_1) = 2776$, $\nu_4(E) = 2706$, and $\nu_6(E) = 586$ cm^{-1} being suggested.[21] In light of the present study and the results of our previous calculations[2,3] on $\tilde{X}^2E$ CH_3O (the methoxy radical CH_3O is an analogue of CH_3S but more extensively studied), some (or all) of these assignments may be incorrect. The value of $\nu_6(E) = 586$ cm^{-1} (ref 21) is significantly underestimated in comparison with the theoretical predictions for the unperturbed harmonic frequency $\omega_6(E) = 943$ cm^{-1} (Table 1) and the lowest 6_1 spin-vibronic level (at 793 cm^{-1}, Table 3). The intervals calculated for the CH_3-stretchings in $\tilde{X}^2E_{3/2}$ CH_3S (in cm^{-1}, see the symmetry notations in Table

2) are 2938 for $1_1(e, e_{3/2}^-)$, 3022 for $4_1(a_1, e_{1/2}^-)$, 3026 for $4_1(e, e_{1/2}^-)$, 3194 for $1_1(e^*, e_{1/2}^+)$, 3275 for $4_1(a_2, e_{1/2}^+)$, and 3282 for $4_1(e^*, e_{3/2}^+)$. They lie much higher than suggested in ref 21. Moreover, the value of $\nu_1(A_1) = 2776$ cm^{-1} (ref 21) is in disagreement with the interval observed in the CH_3S^- anion photoelectron spectrum[34] at 2960 ± 30 cm^{-1} and assigned to the lower spin−orbit component of $1_1(e)$ (cf. 2938 cm^{-1} by theory). The interval at 3225 ± 30 cm^{-1} in ref 34 was assigned to the upper spin−orbit component of $1_1(e^*)$ (3194 cm^{-1} by theory).

The First Excited $\tilde{A}^2A_1$ Electronic State of CH_3S. The EOMIP/aug-cc-pCVTZ values of geometric parameters, harmonic frequencies, and all significant force constants of higher order for $\tilde{A}^2A_1$ CH_3S (Figure 1) are presented in Table 1. The adiabatic energy of the $\tilde{A}^2A_1 \leftrightarrow \tilde{X}^2E_{3/2}$ electronic transition is $T_e = 27\,308$ cm^{-1}. The value of $T_o = 27\,117$ cm^{-1} calculated as a difference of the lowest level energies in the electronic states $\tilde{X}^2E_{3/2}$ and $\tilde{A}^2A_1$ CH_3S is ∼2% overestimated about a wavenumber of the $0_0^0\tilde{A}^2A_1 \rightarrow \tilde{X}^2E_{3/2}$ transition observed in the laser-induced excitation spectra of CH_3S: 26 526.3,[21] 26 529,[22] and 26 531[23] cm^{-1}. In respect to the double C_{3v} symmetry group, the $\tilde{A}^2A_1$ state is correlated to $\tilde{A}^2E_{1/2}$ (Figure 1, part b). There is no spin−orbit coupling between $\tilde{X}^2E$ and $\tilde{A}^2A_1$ CH_3S.

The equilibrium C_{3v} geometries of the ground $\tilde{X}^2E$ and first excited $\tilde{A}^2A_1$ electronic states differ significantly: the value of R_e(C−S) for $\tilde{A}^2A_1$ is larger by 0.27 Å and the value of α_e(HCS) is smaller by 10°. The reason for this is the excitation of an electron from the doubly occupied C−S σ molecular orbital (A_1) to a singly occupied MO of E symmetry interpreted as one of the 3pπ lone pairs localized on the sulfur atom.[1,32] In accordance with the increase of R_e(C−S) in $\tilde{A}^2A_1$ CH_3S, the normal vibration frequency correlated to the CS-stretching decreases: cf. $\omega_3(A_1) = 752$ cm^{-1} for $\tilde{X}^2E$ and $\omega_3(A_1) = 465$ cm^{-1} for $\tilde{A}^2A_1$. A vertical energy of the $\tilde{A}^2A_1 \leftrightarrow \tilde{A}^2E_{3/2}$ transition calculated at the C_{3v} nuclear configuration optimized for $\tilde{X}^2E$ is 31100 cm^{-1} (Figure 1, part b), much higher than $T_e = 27\,308$ cm^{-1}.

To study a possible role of nonadiabatic coupling of the ground $\tilde{X}^2E$ and first excited $\tilde{A}^2A_1$ electronic states of CH_3S, the linear pseudo-Jahn−Teller constants λ_4, λ_5, and λ_6 involved in the terms $V_{\pm\mp}^{PJT} = \sum_{i=4}^{6}\lambda_i Q_{i\mp}$ of the diabatic electronic matrix in eq 6 were calculated numerically by means of least-squares fitting of eqs 7−9 to ab initio values of total energies of three states ($E = A' + A''$ and A_1). Setting the vibrational parameters of ω- and f-type for $\tilde{X}^2E$ CH_3S fixed at values shown in Table 1, we varied all other magnitudes: vibrational parameters ω and f for the $\tilde{A}^2A_1$ state, linear PJT parameters λ, and all the JT constants k and g. The final values of λ_i are $|\lambda_i| \leq 10$ cm^{-1} that gives an extremely small (below the computational accuracy) contribution (A_{PJT}^2/T_v) ≤ 0.003 cm^{-1} to the adiabatic potentials $U_{E(A')}$ and U_{A_1} in eqs 10 and 11 with $T_v = 31\,100$ cm^{-1}. According to the results of CASSCF calculations with the state-averaged density matrix, the adiabatic electronic wave functions $\Psi_{\tilde{X}^2E}$ for the two components of the E-term are dominated by Slater determinants $\Phi_1[(a_1)^2(e_a)^2(e_b)^1(a_1)^0]$ and $\Phi_2[(a_1)^2(e_a)^1(e_b)^2(a_1)^0]$, whereas the $\tilde{A}^2A_1$ state is assigned in terms of a single electron excitation $\Phi_3[(a_1)^1(e_a)^2(e_b)^2(a_1)^0]$. Analysis of these wave functions calculated at the $C_s(A')$ equilibrium geometries corresponding to the Jahn−Teller minimum (Figure 1, part a) shows that the ground $\tilde{X}^2E$ and first excited $\tilde{A}^2A_1$ electronic states are coupled only very weakly by the vibrational distortions:

$$\Psi_{\tilde{X}^2E(A')} = 0.413\Phi_1 + 0.903\Phi_2 + 0.018\Phi_3$$

$$\Psi_{\tilde{X}^2E(A)} = 0.903\Phi_1 - 0.413\Phi_2$$

$$\Psi_{\tilde{A}^2A_1} = -0.007\Phi_1 - 0.016\Phi_2 + 0.993\Phi_3$$

Thus, the terms $V_{\pm\mp}^{PJT} = \sum_{i=4}^{6}\lambda_i Q_{i\mp}$ can be safely removed from the model Hamiltonian and the ground $\tilde{X}^2E$ and first excited $\tilde{A}^2A_1$ electronic states of CH_3S can be treated individually with use of eqs 1 and 5. Couplings of the ground $\tilde{X}^2E$ state to other (higher than $\tilde{A}^2A_1$) excited states are expected to be still smaller. For comparison, vertical energies of the lowest electronic states of the same multiplicity were calculated with the use of multiconfiguration quasi-degenerate second-order perturbation theory: 0 ($\tilde{X}^2E$), 30206 ($\tilde{A}^2A_1$), 46108 ($^2A_2$), and 54 378 (^2E) cm^{-1}.

As known from the literature,[32,33,35,37] the $\tilde{A}^2A_1$ adiabatic surface of CH_3S, like any radical of the methoxy family (CH_3X, CF_3X, X = O, S), correlates asymptotically to $CH_3(\tilde{X}^2A_2'') + S(^1D)$, being crossed by three repulsive surfaces, which belong to the CH_3S states ^4E, $^2A_2$, and $^4A_2$ and correlate to $CH_3(\tilde{X}^2A_2'') + S(^3P)$. According to an ab initio study of the photodissociation of CH_3S by Cui and Morokuma,[37] the energy of intersection between the bonding $\tilde{A}^2A_1$ and first repulsive $^4A_2$ states is only 0.13 eV (1049 cm^{-1}) above the $\tilde{A}^2A_1$ state minimum. The threshold energy for the nonadiabatic predissociative photofragmentation of CH_3S is expected to be lower than for the dissociation CH_3S ($\tilde{A}^2A_1$) → CH_3 ($\tilde{X}^2A_2''$) + S (^1D). The energy of the latter reaction is 0.73 eV.[37] For comparison, the stability of the ground state $\tilde{X}^2E$ in respect to the channel CH_3S ($\tilde{X}^2E$) → CH_3 ($\tilde{X}^2A_2''$) + S (^3P) is 2.93 eV.[37] Experimental evidence of predissociation in $\tilde{A}^2A_1$ CH_3S includes the sharp decrease of radiative lifetimes of the vibrational states for the 3_0^v(v = 1 and 2) transitions relative to 0_0^0 and the absence of the band signal for $v > 2$ in the excitation spectrum.[23] Transitions to the vibrational levels of $\tilde{A}^2A_1$ CH_3S lying above the predissociation threshold (≥800 cm^{-1})[21,23,33] were resolved in the CH_3S photofragment yield spectrum.[33]

The energies of low vibrational levels in $\tilde{A}^2A_1$ CH_3S calculated in the present study are compared to observed intervals in Table 4. Agreement between theory and experiment is somewhat worse in the case of $\tilde{A}^2A_1$ (Table 4) than for $\tilde{X}^2E$ CH_3S (Table 3). A more accurate dynamical calculation should account for the dissociative (predissociative) nature of the vibrational modes in $\tilde{A}^2A_1$ CH_3S. The remaining disagreement between theory and experiment (Tables 3 and 4) is likely to be caused by computational errors in our study (mainly omission of triple- and higher-order excitations in the EOMIP−CCSD method[10] and inaccuracy of the ab initio calculation of spin−orbit splitting in the ground state) and also by uncertainties in experimental measurements and errors in band assignments. With respect to the latter, experiments on CH_3S have not yet provided

Table 4. Theoretical and Observed Vibrational Energy Intervals (in cm^{-1}) in the First Excited Electronic State $\tilde{A}^2A_1$ CH_3S

assignment	theory	experiment[a]
$0^0(A_1)$	0	0
$3^1(A_1)$	452	401 ± 2,[b,c] 403 ± 1,[d] 402[e]
$6^1(E)$	689	635 ± 10[b]
$3^2(A_1)$	905	795,[b,c] 799,[d] 794[e]
$3^16^1(E)$	1134	
$2^1(A_1)$	1165	1098 ± 2[b,c,e]
$6^2(E)$	1342	
$6^2(A_1)$	1367	
$3^3(A_1)$	1369	1181,[b] 1180[c,e]
$5^1(E)$	1446	
$3^26^1(E)$	1585	
$2^13^1(A_1)$	1613	1490,[b] 1489[c]
$3^16^2(E)$	1787	
$3^16^2(A_1)$	1808	
$1^1(A_1)$	3001	2966[c]
$4^1(E)$	3165	

[a] The intervals from the $\tilde{X}^2E_{3/2} \rightarrow \tilde{A}^2A_1$ laser-induced excitation spectra of CH_3S were calculated from the wavelengths of excited bands (3_0^1, 3_0^2, 3_0^3, $2_0^13_0^1$, 6_0^1, and 1_0^1 in refs 21−23 and 36) relative to the origin 0_0^0. [b] Reference 21. [c] Reference 36. [d] Reference 23. [e] Reference 22.

complete and totally reliable data about the structure and transition frequencies of CH_3S, especially for the fundamentals $\nu_1(A_1)$, $\nu_4(E)$, $\nu_5(E)$, $\nu_6(E)$ and relevant overtones. Since the Jahn−Teller coupling in $\tilde{X}^2E$ CH_3S is small, the laser-induced excitation and dispersed fluorescence $\tilde{A}^2A_1 \leftrightarrow \tilde{X}^2E$ transitions (for instance, M_0^1 and M_1^0, respectively) involving excitations of the Jahn−Teller active vibrations ($M = 4-6$) may exhibit very weak intensities unresolved or undetected within the accuracy of measurements. The absence of spectral transitions correlated to the symmetric CH_3-stretching $Q_1(A_1)$ is likely due to unfavorable Franck−Condon factors.[35]

Conclusions

A variational ab initio study of the spin-vibronic dynamics in the ground $\tilde{X}^2E$ and first excited $\tilde{A}^2A_1$ electronic states of CH_3S has been performed for the first time with inclusion of all the important anharmonic effects and higher-order Jahn−Teller couplings and with account for the vibrational and vibronic interactions between different normal modes. The electronic problem has been solved with use of the equation-of-motion coupled cluster method and augmented basis sets of triple-ζ quality. A nonadiabatic coupling of the ground $\tilde{X}^2E$ and first excited $\tilde{A}^2A_1$ electronic states is shown to be small, which validates the adiabatic separation of these two states for studying the nuclear motion. However, unlike the case of $\tilde{A}^2A_1$, the nuclear dynamics in $\tilde{X}^2E$ CH_3S simultaneously affected by two components of the degenerate electronic state has been studied here beyond the adiabatic Born−Oppenheimer approximation that is broken down by the Jahn−Teller effect. The Jahn−Teller stabilization energy and barrier to pseudorotation are $E_{JT} = 92$ cm^{-1} and $\Delta_{JT} = 15$ cm^{-1}, respectively. The Jahn−Teller distortions of the CH_3S high symmetry nuclear configuration are totally quenched by a relatively strong spin−orbit coupling ($-A_{SO}\xi_e = 358$ cm^{-1}). Nevertheless, the remaining spin-vibronic coupling still makes a heavy impact on the spectroscopic properties of the CH_3S radical.

Despite the growth of computational capacities during the last two decades, there is a distinct lack of explicit ab initio calculations of vibronic or spin-vibronic spectra (see refs 7 and 8 for calculations on the methoxy radical $\tilde{X}^2E$ CH_3O and the methoxy family of radicals, see also references in refs 6 and 19 on other types of vibronic systems). The methylthio radical CH_3S is an important intermediate in environmental chemistry.[21] Hence, an accurate prediction of its molecular properties is critical for practical applications. The agreement between theory and available experimental data is considered as good, especially for the theoretical model using no empirical adjustments. Results of calculations within the complete set of vibrational modes predict spin-vibronic intervals never observed in experiment and significantly supplement the spectroscopic data presently available in the literature.[38] Theoretical predictions presented here can be used for interpretations of results of future CH_3S spectroscopy studies.

Acknowledgment. We are grateful to John Stanton for an opportunity to use his expanded version of the ACESII program and wish to thank Pablo Garcia Fernandez and Xinzheng Yang (Austin, Texas) for discussing the manuscript. Acknowledgments are made to the Donors of the ACS Petroleum Research Fund and to the Welch Foundation (Grant F-100) for support of this research. It is also a part of Project No. 2000-013-1-100 of the IUPAC entitled "Selected Free Radicals and Critical Intermediates: Thermodynamic Properties from Theory and Experiment" (inquiries to T. Berces, berces@chemres.hu).

References

(1) Marenich, A. V.; Boggs, J. E. *J. Phys. Chem. A* **2004**, *108*, 10594−10601.

(2) Marenich, A. V.; Boggs, J. E. *J. Chem. Phys.* **2005**, *122*, 024308/1−024308/11.

(3) Marenich, A. V.; Boggs, J. E. *Chem. Phys. Lett.* **2005**, *404*, 351−355.

(4) Bunker, P. R.; Jensen, P. *Molecular Symmetry and Spectroscopy*, 2nd ed.; NRC Research: Ottawa, Canada, 1998.

(5) Flurry, R. L., Jr. *Symmetry Groups*; Prentice-Hall: Englewood Cliffs, NJ, 1980.

(6) Bersuker, I. B. *Chem. Rev.* **2001**, *101*, 1067−1114.

(7) Barckholtz, T. A.; Miller, T. A. *Int. Rev. Phys. Chem.* **1998**, *17*, 435−524.

(8) Höper, U.; Botschwina, P.; Köppel, H. *J. Chem. Phys.* **2000**, *112*, 4132−4142.

(9) Sliznev, V. V. Private communication. Solomonik, V. G. Doctor in Chemistry Thesis, Moscow State University, 1993.

(10) Stanton, J. F.; Gauss, J. *J. Chem. Phys.* **1994**, *101*, 8938−8944.

(11) Dunning, T. H., Jr. *J. Chem. Phys.* **1989**, *90*, 1007−1023. Kendall, R. A.; Dunning, T. H., Jr.; Harrison, R. J. *J. Chem. Phys.* **1992**, *96*, 6796−6806. Woon, D. E.; Dunning, T. H., Jr. *J. Chem. Phys.* **1993**, *98*, 1358−1371. Basis sets were obtained from the Extensible Computational Chemistry

Environment Basis Set Database, Version 02/25/04, as developed and distributed by the Molecular Science Computing Facility, Environmental and Molecular Sciences Laboratory which is part of the Pacific Northwest Laboratory, P.O. Box 999, Richland, WA 99352, U.S.A., and funded by the U.S. Department of Energy. The Pacific Northwest Laboratory is a multiprogram laboratory operated by Battelle Memorial Institute for the U.S. Department of Energy under contract DE-AC06-76RLO 1830. Contact Karen Schuchardt for further information.

(12) Woon, D. E.; Dunning, T. H., Jr. *J. Chem. Phys.* **1995**, *103*, 4572−4585. Peterson, K. A.; Dunning, T. H., Jr. *J. Chem. Phys.* **2002**, *117*, 10548−10560.

(13) Stanton, J. F.; Gauss, J.; Watts, J. D.; Lauderdale, W. J.; Bartlett, R. J. *Int. J. Quantum Chem., Quantum Chem. Symp.* **1992**, *26*, 879−894.

(14) Nakano, H. *J. Chem. Phys.* **1993**, *99*, 7983−7992.

(15) Fedorov, D. G.; Koseki, S.; Schmidt, M. W.; Gordon, M. S. *Int. Rev. Phys. Chem.* **2003**, *22*, 551−592.

(16) Schmidt, M. W.; Baldridge, K. K.; Boatz, J. A.; Elbert, S. T.; Gordon, M. S.; Jensen, J. H.; Koseki, S.; Matsunaga, N.; Nguyen, K. A.; Su, S. J.; Windus, T. L.; Dupuis, M.; Montgomery, J. A. *J. Comput. Chem.* **1993**, *14*, 1347−1363.

(17) Woywod, C.; Scharfe, S.; Krawczyk, R.; Domcke, W.; Köppel, H. *J. Chem. Phys.* **2003**, *118*, 5880−5893.

(18) Mahapatra, S.; Vallet, V.; Woywod, C.; Köppel, H.; Domcke, W. *Chem. Phys.* **2004**, *304*, 17−34.

(19) Köppel, H. *Adv. Ser. Phys. Chem.* **2004**, *15*, 429−472.

(20) Haller, E.; Köppel, H.; Cederbaum, L. S.; von Niessen, W.; Bieri, G. *J. Chem. Phys.* **1983**, *78*, 1359−1370.

(21) Chiang, S.-Y.; Lee, Y.-P. *J. Chem. Phys.* **1991**, *95*, 66−72.

(22) Misra, P.; Zhu, X.; Bryant, H. L., Jr. *Pure Appl. Opt.* **1995**, *4*, 587−598.

(23) Suzuki, M.; Inoue, G.; Akimoto, H. *J. Chem. Phys.* **1984**, *81*, 5405−5412.

(24) Callear, A. B.; Dickson, D. R. *Trans. Faraday Soc.* **1970**, *66*, 1987−1995.

(25) Ohbayashi, K.; Akimoto, H.; Tanaka, I. *Chem. Phys. Lett.* **1977**, *52*, 47−49.

(26) Engelking, P. C.; Ellison, G. B.; Lineberger, W. C. *J. Chem. Phys.* **1978**, *69*, 1826−1832.

(27) Janousek, B. K.; Brauman, J. I. *J. Chem. Phys.* **1980**, *72*, 694−700.

(28) Black, G.; Jusinski, L. E. *J. Chem. Soc., Faraday Trans. 2* **1986**, *82*, 2143−2151.

(29) Endo, Y.; Saito, S.; Hirota, E. *J. Chem. Phys.* **1986**, *85*, 1770−1777.

(30) Hsu, Y.-C.; Liu, X.; Miller, T. A. *J. Chem. Phys.* **1989**, *90*, 6852−6857.

(31) Anastasi, C.; Broomfield, M.; Nielsen, O. J.; Pagsberg, P. *Chem. Phys. Lett.* **1991**, *182*, 643−648.

(32) Hsu, C.-W.; Liao, C.-L.; Ma, Z.-X.; Tjossem, P. J. H.; Ng, C. Y. *J. Chem. Phys.* **1992**, *97*, 6283−6290.

(33) Bise, R. T.; Choi, H.; Pedersen, H. B.; Mordaunt, D. H.; Neumark, D. M. *J. Chem. Phys.* **1999**, *110*, 805−816.

(34) Schwartz, R. L.; Davico, G. E.; Lineberger, W. C. *J. Electron. Spectrosc. Relat. Phenom.* **2000**, *108*, 163−168.

(35) Pushkarsky, M. B.; Applegate, B. E.; Miller, T. A. *J. Chem. Phys.* **2000**, *113*, 9649−9657.

(36) Liu, C.-P.; Matsuda, Y.; Lee, Y.-P. *J. Chem. Phys.* **2003**, *119*, 12335−12341.

(37) Cui, Q.; Morokuma, K. *Chem. Phys. Lett.* **1996**, *263*, 54−62.

(38) Jacox, M. E. *J. Phys. Chem. Ref. Data* **2003**, *32*, 1−441.

CT0501452